

Examination and experimental constraints of the stellar reaction rate factor $N_A < \sigma v >$ of the $^{18}\text{Ne}(\alpha,p)^{21}\text{Na}$ reaction at temperatures of X-Ray Bursts

P. Mohr^{1,2,*} and A. Matic^{3,†}

¹ Diakonie-Klinikum, D-74523 Schwäbisch Hall, Germany

² Institute of Nuclear Research (ATOMKI), H-4001 Debrecen, Hungary

³ Kernfysisch Versneller Instituut, University of Groningen, Zernikelaan 25, NL-9747 AA Groningen, The Netherlands

(Dated: July 20, 2018)

The $^{18}\text{Ne}(\alpha,p)^{21}\text{Na}$ reaction is one key for the break-out from the hot CNO-cycles to the rp -process. Recent papers have provided reaction rate factors $N_A < \sigma v >$ which are discrepant by at least one order of magnitude. The compatibility of the latest experimental results is tested, and a partial explanation for the discrepant $N_A < \sigma v >$ is given. A new rate factor is derived from the combined analysis of all available data. The new rate factor is located slightly below the higher rate factor by Matic *et al.* at low temperatures and significantly below at higher temperatures whereas it is about a factor of five higher than the lower rate factor recently published by Salter *et al.*

PACS numbers: 25.60.-t, 25.55.-e, 26.30.-k

I. INTRODUCTION

The reaction rate of the $^{18}\text{Ne}(\alpha,p)^{21}\text{Na}$ reaction provides a route from hot CNO-cycles to the NeNa and MgAl cycles and finally to the rp -process at typical temperatures of e.g. about 1–2 GK ($T_9 = 1–2$) in X-ray bursters (XRB) [1]. It is expected that this reaction is the dominating route in the low temperature range [2]. An alternative route from hot CNO-cycles to the rp -process may be the $^{15}\text{O}(\alpha,\gamma)^{19}\text{Ne}$ reaction.

The relatively high temperatures correspond to most effective energies of about 1.3 to 2.1 MeV for the $^{18}\text{Ne}(\alpha,p)^{21}\text{Na}$ reaction which are experimentally well accessible. However, experiments remain very difficult because of the short-living ^{18}Ne nucleus ($T_{1/2} = 1.67\text{s}$) and the limited intensity of radioactive beam facilities. Thus, besides the direct approach of measuring the $^{18}\text{Ne}(\alpha,p)^{21}\text{Na}$ reaction cross section [3, 4], the reverse $^{21}\text{Na}(p,\alpha)^{18}\text{Ne}$ reaction has been studied very recently [5] and in an earlier unpublished experiment [6], and the resonance energies have been determined from various transfer experiments populating states in the compound ^{22}Mg nucleus [7–11].

The focus of the present paper is the comparison of the latest experiments by Groombridge *et al.* (hereafter: GRO) [4], Salter *et al.* (SAL) [5], Chae *et al.* (CHA) [10], and Matic *et al.* (MAT) [11]. The earlier direct data of [3] have been improved and extended by the same group leading to the GRO data. The SAL data are the only published data for the inverse reaction; a brief comparison to the unpublished data measured at Argonne National Laboratory (ANL) is also provided. The MAT transfer data have by far the best energy resolution which is essential for a precise determination of the resonance

energies. Additional measurements of angular distributions in CHA lead to a new spin assignment only in few cases (see Table III of CHA).

The reaction rate factor $N_A < \sigma v >$ for the $^{18}\text{Ne}(\alpha,p)^{21}\text{Na}$ reaction is given by the sum over the contributing resonances:

$$\frac{N_A < \sigma v >}{\text{cm}^3 \text{s}^{-1} \text{mol}^{-1}} = 1.54 \times 10^{11} (\mu T_9)^{-3/2} \times \sum_i (\omega\gamma)_i \times \exp(-11.605 E_i / T_9) \quad (1)$$

with the reduced mass μ in units of amu, the resonance energies E_i in MeV, and the resonance strengths $(\omega\gamma)_i$ in MeV. In general, resonance energies are given as E in the center-of-mass (c.m.) system without index; excitation energies are given as E^* in this paper.

The resonance strength $(\omega\gamma)$ for the $^{18}\text{Ne}(\alpha,p)^{21}\text{Na}$ reaction is given by

$$\omega\gamma = (2J+1) \frac{\Gamma_\alpha \Gamma_p}{\Gamma} \quad (2)$$

with the resonance spin J , the partial widths Γ_α and Γ_p , and the total width $\Gamma = \Gamma_\alpha + \Gamma_p + \Gamma_\gamma \approx \Gamma_\alpha + \Gamma_p$. In most cases it can be expected that $\Gamma_\alpha \ll \Gamma_p$, and thus $(\omega\gamma) \approx (2J+1) \Gamma_\alpha$. The application of the simple formula for narrow resonances in Eq. (1) is justified because the resonance widths Γ are much smaller than the resonance energies E [12].

In the following we first briefly review the various experimental approaches and discuss the resulting uncertainties in the determination of the reaction rate factor $N_A < \sigma v >$. Next we check whether the experimental results of GRO, MAT, CHA, SAL, and ANL are compatible with each other. Finally, the reaction rate factors $N_A < \sigma v >$ of the different studies are compared. Note that $N_A < \sigma v >$ of different studies may differ not only from discrepant resonance energies and resonance strengths or cross sections, but also from a different number of considered resonances in Eq. (1).

*Email: WidmaierMohr@t-online.de

†Present address: IBA Particle Therapy, D-45157 Essen, Germany

II. BRIEF REVIEW OF AVAILABLE DATA

A. Transfer data

Various transfer experiments have been performed in the last decade to study properties of the compound nucleus ^{22}Mg [7–11]. A detailed comparison of the results is provided in MAT and is not repeated. Here we briefly summarize the MAT results and some modifications resulting from the CHA data.

Transfer data are able to provide excitation energies E^* and spin and parity J^π of states in ^{22}Mg . However, from the transfer data it is not possible to determine resonance strengths $\omega\gamma$ which are the second ingredient for the calculation of the rate factor $N_A \langle \sigma v \rangle$ in Eq. (1).

1. Matic et al.

In the MAT approach the $^{24}\text{Mg}(p,t)^{22}\text{Mg}$ reaction is used to populate excited states in the compound nucleus ^{22}Mg at proton energies of slightly below 100 MeV. The experiment has been performed using the Grand Raiden spectrometer at RCNP, Osaka. The excellent energy resolution of about 13 keV allows a precise determination of excitation energies E^* which enter exponentially into $N_A \langle \sigma v \rangle$ in Eq. (1) via $E^* = E + S_\alpha$ (with the separation energy of the α particle in ^{22}Mg of $S_\alpha = 8.142$ MeV) and are thus the main source of uncertainties. ($S_\alpha = 8.142$ MeV is taken from the new Audi and Meng compilation [13]; the small difference to the earlier result of $S_\alpha = 8.139$ MeV [14] does practically not affect the rate factor $N_A \langle \sigma v \rangle$ in the relevant temperature range around $T_9 = 1 - 2$.)

In addition to the excitation energies E^* , the total widths Γ can be determined from these data by fitting the observed peak widths Γ_{obs} . Most of the observed states are much broader than the experimental resolution, and thus the required unfolding procedure leads only to minor additional uncertainties for the derived width Γ . The results are listed in Table I. As can be seen from Table I, practically all resonances fulfill the criterion of $\Gamma/E \leq 0.1$ which is often used as definition for narrow resonances (although also more stringent definitions for narrow resonances can be found in literature). As we will show in Sect. II A 2, the simple formula for narrow resonances in Eq. (1) provides the reaction rate factor $N_A \langle \sigma v \rangle$ for the $^{18}\text{Ne}(\alpha,p)^{21}\text{Na}$ reaction with sufficient accuracy. In this sense the resonances in Table I can be considered generally as narrow resonances.

The resonance strengths $\omega\gamma$ in MAT have generally been calculated by the following procedure. In a first step spin and parity J^π for the states seen in the $^{24}\text{Mg}(p,t)^{22}\text{Mg}$ experiment were tentatively assigned from the mirror nucleus ^{22}Ne . Note that the level scheme for the stable mirror nucleus ^{22}Ne is well-established up to relatively high excitation energies. In some cases also theoretical predictions from the shell model have been

TABLE I: Excitation energy E^* , resonance energy E , spin and parity J^π , total width Γ , and resonance strength $\omega\gamma$ for excited states in ^{22}Mg from the $^{24}\text{Mg}(p,t)^{22}\text{Mg}$ experiment in [11]. Later revisions for individual states are marked by “*GRO” and “*CHA”; these revisions are based on the replacement of the experimental resonance strengths of GRO by calculated resonance strengths and on revised (but still tentative) spin assignments by CHA [10] (see also Table II). The finally recommended strengths will be slightly lower by a factor of 0.55 (see discussion in Sect. III B and IV).

E^* (MeV)	E (MeV)	J^π	Γ (keV)	$\omega\gamma$ (eV)
8.182	0.040	[2 ⁺]	33.5±2.2	8.53×10 ⁻⁶⁵
8.385	0.243	[2 ⁺]	47.0±5.3	1.33×10 ⁻¹⁷
8.519	0.377	[3 ⁻]	25.7±4.1	4.87×10 ⁻¹⁴ *CHA
8.574	0.432	[4 ⁺]	20.6±16.8	3.26×10 ⁻¹²
8.657	0.515	[0 ⁺]	15.5±3.5	4.97×10 ⁻⁸
8.743	0.601	[4 ⁺]	65.5±22.8	5.15×10 ⁻⁹
8.783	0.641	[1 ⁻]	22.5±7.0	1.21×10 ⁻⁵
8.932	0.790	[2 ⁺]	51.6±5.9	4.13×10 ⁻⁴
9.080	0.938	[1 ⁻]	114.4±19.7	2.31×10 ⁻²
9.157	1.015	[4 ⁺]	< 20.5	8.70×10 ⁻⁴
9.318	1.176	[2 ⁺]	22.6±8.0	4.97×10 ⁻¹
9.482	1.340	[3 ⁻]	< 6.3	1.25×10 ⁻¹
9.542	1.400	[2 ⁺]	< 22.9	1.78×10 ⁰ *CHA
9.709	1.567	[0 ⁺]	267.8±48.2	5.18×10 ¹
9.752	1.610	[2 ⁺]	31.4±6.8	8.22×10 ⁰ *CHA
9.860	1.718	[0 ⁺]	121.3±10.4	2.07×10 ¹
10.085	1.943	[2 ⁺]	25.8±9.3	2.25×10 ²
10.272	2.130	2 ⁺	20.7±2.7	1.03×10 ⁴ *GRO
10.429	2.287	[4 ⁺]	144.2±25.8	7.30×10 ³ *GRO
10.651	2.509	[3 ⁻]	72.8±19.1	1.82×10 ⁴ *GRO
10.768	2.626	[2 ⁺]	94.9±29.6	1.16×10 ⁴
10.873	2.731	[0 ⁺]	40.2±12.0	4.52×10 ⁴ *GRO
11.001	2.859	[4 ⁺]	135.8±12.9	8.10×10 ³ *GRO
11.315	3.173	[4 ⁺]	203.7±37.0	1.83×10 ³
11.499	3.357	[2 ⁺]	116.8±21.8	8.64×10 ⁴
11.595	3.453	[1 ⁻]	48.3±14.7	6.11×10 ⁴ *CHA
11.747	3.605	[0 ⁺]	166.1±64.4	7.13×10 ⁴
11.914	3.772	[0 ⁺]	122.4±19.7	8.82×10 ⁴ *CHA
12.003	3.861	[1 ⁻]	— ^a	4.31×10 ⁵
12.185	4.043	[3 ⁻]	236.4±52.0	2.60×10 ⁵
12.474	4.332	[2 ⁺]	193.8±51.6	3.89×10 ⁵
12.665	4.523	[3 ⁻]	128.8±23.5	3.45×10 ⁵
13.010	4.868	[0 ⁺]	600.9±114.5	2.16×10 ⁵

^astate adopted from [9]

used [15]. Next, upper limits for Γ_α were calculated from the single-particle Wigner limit using the tentative spin assignments (see Table VII in MAT, partly repeated in Table I in this work). Finally, the Wigner limit has been scaled by carefully chosen reduced widths. Whenever possible, the reduced α -widths were taken from experimental data obtained for the stable mirror nucleus ^{22}Ne by α -transfer on the mirror target ^{18}O . In the remaining cases where no experimental information is available, the reduced α -widths were estimated by simple but reasonable theoretical assumptions. A detailed discussion is given in Sect. V in MAT.

In the few cases where experimental data are available

from the GRO study, experimental resonance strengths were used by MAT in their calculation of $N_A \langle \sigma v \rangle$. Levels from threshold up to an excitation energy of about 13 MeV (corresponding to $E \approx 5$ MeV) are taken into account in MAT (see their Table VII), and thus the resulting rate factor $N_A \langle \sigma v \rangle$ is well determined over a broad temperature range including the astrophysically most relevant range of $T_9 = 1 - 2$.

For an independent comparison of the various studies of the $^{18}\text{Ne}(\alpha, p)^{21}\text{Na}$ reaction, we replace the experimental resonance strengths from the GRO data by calculations similar to the other resonance strengths in MAT (see upper part of Table II; these data will be referenced as MAT-th: “th” for theoretical strengths only). A further explanation for this replacement will become visible later in the comparison of the MAT data to the GRO data and SAL data (see Sect. III C).

TABLE II: Revisions for resonance strengths $\omega\gamma$, compared to Table VII in MAT and Table I. The upper five lines are recalculations of $\omega\gamma$ instead of the resonance strengths adopted from GRO (here $\omega\gamma_{\text{MAT}}$ is identical to $\omega\gamma_{\text{GRO}}$). The lower five lines result from new spin assignments in CHA. For comparison, the original strengths $\omega\gamma_{\text{MAT}}$ from MAT are also listed.

E^* (MeV)	E (MeV)	J^π	$\omega\gamma$ (eV)	$\omega\gamma_{\text{GRO}}$ (eV)
10.272	2.130	2^+	1.31×10^3	1.03×10^4
10.429	2.287	$[4^+]$	4.89×10^1	7.30×10^3
10.651	2.509	$[3^-]$	1.12×10^3	1.82×10^4
10.873	2.731	$[0^+]$	1.19×10^4	4.52×10^4
11.001	2.859	$[4^+]$	5.81×10^2	8.10×10^3

E^* (MeV)	E (MeV)	J^π	$\omega\gamma$ (eV)	$\omega\gamma_{\text{MAT}}$ (eV)	J_{MAT}^π
8.519	0.377	$[2^+]$	1.53×10^{-11}	4.87×10^{-14}	$[3^-]$
9.542	1.400	$[1^-]$	1.31×10^1	1.78×10^0	$[2^+]$
9.752	1.610	$[1^-]$	4.82×10^1	8.22×10^0	$[2^+]$
11.595	3.453	$[4^+]$	3.67×10^3	6.11×10^4	$[1^-]$
11.914	3.772	$[2^+]$	1.77×10^5	8.82×10^4	$[0^+]$

Under the realistic assumption that the total width Γ is dominated by the proton partial width Γ_p (and thus $\omega\gamma \approx \omega\Gamma_\alpha$ and $\Gamma \approx \Gamma_p$), the reaction cross section $\sigma(E)$ as a function of energy can be calculated as a sum over Breit-Wigner resonances: $\sigma(E) = \sum_i \sigma_{\text{BW},i}(E)$ with

$$\sigma_{\text{BW}}(E) = \frac{\pi \hbar^2}{2\mu E} \frac{\omega\Gamma_\alpha\Gamma_p}{(E - E_R)^2 + \Gamma^2/4} \quad (3)$$

The result is shown in Fig. 1 (MAT-th, thin dotted black line). The upper limit of the total width Γ has been used for the three resonances at $E^* = 9.157, 9.482,$ and 9.542 MeV. The resulting uncertainty from these upper limits for the reaction rate factor $N_A \langle \sigma v \rangle$ remains negligible because the resonances are narrow in any case.

This calculation of the cross section $\sigma(E)$ enables a more detailed comparison of the data from transfer and from the study of the inverse reaction (see Sect. III B). The original strengths of MAT (using the experimental GRO strengths where available) lead to the green short-dashed curve in Fig. 1 which is much higher at ener-

gies between 2 and 3 MeV because of the high resonance strengths taken from the GRO data.

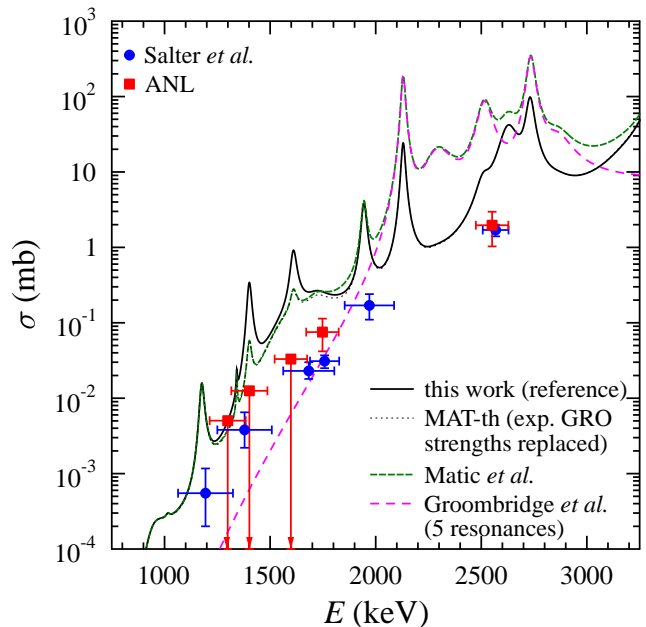


FIG. 1: (Color online) Reaction cross section of the $^{18}\text{Ne}(\alpha, p)^{21}\text{Na}$ reaction, calculated from total widths Γ (see Table I) and from resonance strengths $\omega\gamma$. The full black line uses the MAT strengths with all revisions in Table II (reference cross section σ_{ref}). The green short-dashed line refers to the original MAT strengths (from their Table VII). The long-dashed magenta line shows the five GRO resonances only. The black dotted line (MAT-th) uses the MAT strengths but replaces the experimental GRO strengths by the calculated strengths (see first five lines in Table II). MAT-th is almost identical to MAT (green short-dashed) at low energies and to σ_{ref} (full black) at higher energies; thus, the black dotted MAT-th curve becomes only visible at energies around $E \approx 1.8$ MeV. The experimental data points have been determined by the inverse $^{21}\text{Na}(p, \alpha)^{18}\text{Ne}$ reaction and represent the ground state contribution only. Further discussion see text.

2. Chae et al.

The CHA data are also based on a study of the $^{24}\text{Mg}(p, t)^{22}\text{Mg}$ reaction. The experiment has been performed at lower energies slightly above 40 MeV at the Holifield Radioactive Ion Beam Facility at Oak Ridge. The achieved energy resolution does not reach the MAT data, but the larger angular range under study allows an improved but still tentative assignment of spin and parity J^π of several states in ^{22}Mg .

We have taken the tentative assignments from the CHA data and have recalculated the resonance strengths $\omega\gamma$ for these states using the adopted energies of the high-resolution MAT data. The results are listed in Table II (lower part). The new spin assignments lead to smaller

spins J for some low-lying resonances and consequently to larger resonance strengths $\omega\gamma$ because of the reduced centrifugal barrier. However, the rate factor $N_A < \sigma v >$ is given as the sum over many resonances, and the influence of the new spin assignments on the total rate factor remains below a factor of two over the astrophysically relevant temperature range of $T_9 = 1 - 2$.

The calculated resonance strengths $\omega\gamma$ from Table VII in MAT with all modifications from Table II are taken as a reference in this work to calculate $\sigma_{\text{ref.}}(E)$ and the rate factor $N_A < \sigma v >_{\text{ref.}}$. For simplicity, the rate factor $N_A < \sigma v >$ has been calculated from the approximation in Eq. (1). Thus, it will also be possible to modify our rate factor without much efforts as soon as improved experimental data for any of the $^{18}\text{Ne}(\alpha,p)^{21}\text{Na}$ resonances will become available. The result is shown as the full black line in Fig. 1. Note that the final recommendation for $\sigma(E)$ and $N_A < \sigma v >$ from the combined analysis of all available experimental data will be almost a factor of 2 lower (see Sect. IV).

We have tested the validity of the simple rate formula for narrow resonances in Eq. (1) by a numerical integration of the $\sigma_{\text{ref.}}(E)$ curve, and it is found that the deviation between the numerical integration and the simple formula in Eq. (1) remains below 10% over the full temperature range under study ($T_9 = 0.25 - 3$) and far below 5% for the most relevant range of $T_9 = 1 - 2$.

It is obvious that the calculated cross section $\sigma(E)$ and reaction rate factor $N_A < \sigma v >$ depend on the spin and parity J^π of the considered resonances. A detailed study of the corresponding uncertainties has already been given in MAT using random spin assignments, and it was concluded that $N_A < \sigma v >$ does not change by more than one order of magnitude. Here we provide reduction factors $\Gamma_{s.p.}(L=0)/\Gamma_{s.p.}(L)$ for angular momenta $0 \leq L \leq 4$ in the energy range between 1 and 4 MeV (see Table III) where the α single-particle widths $\Gamma_{s.p.}$ have been calculated similar to MAT. The largest reduction factors are found for large angular momenta L at low energies where the influence of the centrifugal barrier is most important. Here an increase of L by 1 leads to a reduction of a factor of 10 whereas at higher energies and small L the increase of 1 leads to a reduction of less than a factor of 2.

TABLE III: Reduction factors $\Gamma_{s.p.}(L=0)/\Gamma_{s.p.}(L)$ for angular momenta $0 \leq L \leq 4$ in the energy range between 1 and 4 MeV.

E (MeV)	$L=0$	$L=1$	$L=2$	$L=3$	$L=4$
1.0	$\equiv 1.0$	1.9	7.0	44.4	463.1
2.0	$\equiv 1.0$	1.7	5.1	23.8	171.1
3.0	$\equiv 1.0$	1.5	3.4	11.8	60.9
4.0	$\equiv 1.0$	1.3	2.2	5.6	20.9

The assignment of spin and parity J^π of the states in ^{22}Mg (e.g. in MAT) is tentative and has mainly been made from the mirror nucleus ^{22}Ne . Even if some of the individual assignments may be incorrect, the distribution

of spins should be correct because the J^π assignments in ^{22}Ne are mainly firm and not tentative. The cross section $\sigma(E)$ of the $^{18}\text{Ne}(\alpha,p)^{21}\text{Na}$ reaction is composed of overlapping resonances, and the calculation of the rate factor $N_A < \sigma v >$ requires folding with the Maxwell-Boltzmann distribution. Thus, at any astrophysically relevant temperature $T_9 > 1$ the rate factor is defined by a sum over several contributing resonances, and the influence of a modified spin assignment of an individual resonance remains very limited, in particular, if the spin distribution is kept; i.e., the modification of J^π of one resonance (e.g. increase of L and reduced Γ_α and $\omega\gamma$) is compensated by a similar modification of J^π of another resonance (decrease of L and enhanced Γ_α and $\omega\gamma$).

As we will see later, the modified spin assignments of the CHA experiment (mainly smaller J^π than used by MAT, see Table II, lower part) will lead to a marginal enhancement of the rate factor $N_A < \sigma v >$ around $T_9 \approx 1$ by less than a factor of 2. In combination with the above arguments, it seems thus reasonable that the uncertainty of the spin assignments for the calculated rate factor $N_A < \sigma v >$ does not exceed a factor of two in the full temperature range under study.

B. Direct data

The GRO experiment has been performed at the Radioactive Ion Beam facility at Louvain-la-Neuve. They have measured the $^{18}\text{Ne}(\alpha,p)^{21}\text{Mg}$ reaction directly using an extended ^4He gas target and a ^{18}Ne beam. The chosen detection technique allowed the reconstruction of the interaction vertex in the extended gas target, and together with the measured proton energy it was possible to determine the energies and resonance strengths of 8 resonances and their main decay branch into the p_i channel (p_0 corresponds to the ^{21}Na ground state, p_1 to the first excited state, and so on). The data cover the energy range from about 1.7 to 2.9 MeV. The rate factor $N_A < \sigma v >$ was calculated from these 8 resonances; this $N_A < \sigma v >$ is considered as a lower limit by GRO because of the missing resonances outside the studied energy region and because of perhaps missed weak resonances or missed weak branches of observed resonances inside the studied energy region.

The cross section $\sigma(E)$ as a function of energy is calculated from 5 adopted resonances (see discussion below in Sect. III A) using excitation energies E^* from MAT, total widths Γ from Table I, and resonance strengths $\omega\gamma$ from GRO. The result is shown in Fig. 1 with a long-dashed magenta line. Obviously, in the energy region between 2 and 3 MeV it is close to the MAT result because MAT have used resonance strengths from GRO, but it is much higher than the reference calculation of this work.

Finally, it is interesting to note that the summed p_0 resonance strength to the ground state is about 42% of the total summed strength in the GRO data. This number will be relevant for comparison with the SAL and

ANL data for the inverse $^{21}\text{Na}(p,\alpha)^{18}\text{Ne}$ reaction.

C. Data for the inverse reaction

The latest experiment by SAL and the unpublished ANL experiment have used the reverse $^{21}\text{Na}(p,\alpha)^{18}\text{Ne}$ reaction in inverse kinematics with a radioactive ^{21}Na beam and a solid CH_2 target. An average cross section $\bar{\sigma}$ at the energy E_{eff} is determined from the measured α yield:

$$\bar{\sigma}(E_{\text{eff}}) = \frac{1}{2\Delta E} \int_{E_{\text{eff}}-\Delta E}^{E_{\text{eff}}+\Delta E} \sigma(E) dE \quad (4)$$

where E_{eff} is the energy in the center of the CH_2 target, and the total energy loss in the target is given by $2\Delta E$. In the energy range under study the $^{21}\text{Na}(p,\alpha)^{18}\text{Ne}$ cross section populates mainly the ^{18}Ne ground state (no event to the first excited state in ^{18}Ne is observed by SAL). Thus, the measured $^{21}\text{Na}(p,\alpha)^{18}\text{Ne}$ cross section can be converted to the $^{18}\text{Ne}(\alpha,p_0)^{21}\text{Na}_{\text{g.s.}}$ cross section using detailed balance.

Because of the relatively thick targets that are used in the reverse reaction experiments, the energy of each data point is not very well defined. This leads to major uncertainties in the calculation of the reaction rate factor $N_A < \sigma v >$. For example, for the lowest data point of SAL one finds a variation of the astrophysical S-factor of a factor of 5 if the given cross section is converted to the S-factor at the upper or lower energy limit of the data point. Therefore a different way for the comparison of rate factors from the various experimental techniques has been chosen in this work (see Fig. 2 and discussion of Eq. (5) in Sect. III B).

1. Salter et al.

The SAL experiment used the ISAC II facility at TRIUMF. The energy range under study by SAL for the (α,p) reaction (from about 1 MeV up to about 2.6 MeV) extends the energy range of GRO down to lower energies and reaches the Gamow window of the $^{18}\text{Ne}(\alpha,p)^{21}\text{Na}$ reaction for the first time. The SAL data are shown in Fig. 1 as blue points.

From the average cross sections of the (α,p_0) reaction the rate factor $N_A < \sigma v >$ is calculated in SAL using the EXP2RATE code [16]. Because of the missing contributions of the $(\alpha,p_{i \neq 0})$ channels this $N_A < \sigma v >$ is also considered as a lower limit in SAL. These missing contributions are estimated in SAL from Hauser-Feshbach (HF) calculations by T. Rauscher. The calculations indicate that the total rate factor $N_A < \sigma v >$ is about a factor of three larger than the measured ground-state contribution.

The validity of HF calculations is somewhat uncertain in the present case because of the relatively small level

density in the compound nucleus ^{22}Mg . However, this uncertainty mainly influences the absolute value of the calculated cross section which depends on the number of states (or resonances) at the energy under study. The calculation of the decay branches in the proton channel to the ground state and to excited states in ^{21}Na should be less affected because it is dominated by the transmission coefficients. It can also be checked “by hand” by calculating single-particle limits for the proton decay of states in ^{22}Mg . It is found that e.g. the decay of a hypothetical 0^+ state in ^{22}Mg at $E^* = 9.942 \text{ MeV}$ ($E = 1.8 \text{ MeV}$, i.e. in the center of the analyzed energy region of Fig. 1) by proton emission proceeds by 31 % to the ground state of ^{21}Na and by 69 % to excited states. This confirms the HF approach for the decay branch. A further confirmation is obtained from comparison with the GRO data. Here it is found experimentally that the ground state branch contributes with 42 % to the summed strength.

2. ANL data

A similar experiment has also been performed at the Argonne National Laboratory (ANL). Unfortunately, these data have never been published and can be found in the ANL Annual Report only [6]. The data (extracted from the figure in [6]) are shown in Fig. 1 as red squares.

The ANL data point at the highest energy agrees well with SAL. A second data point at lower energies is about a factor of two higher, and the error bars of ANL and SAL are close to overlap. Three upper limits have been determined at lower energies; these upper limits are slightly higher than the SAL data points. In total, the unpublished ANL data are in reasonable agreement with the SAL data.

As usual, it is very difficult to estimate the reliability of unpublished data, and thus a publication of the ANL data would be very helpful. The ANL data do not enter directly into the recommended rate (see Sect. IV), but the reasonable agreement with SAL strengthens the validity of the experimental data by SAL.

III. COMPATIBILITY OF RESULTS FROM VARIOUS EXPERIMENTAL TECHNIQUES

In this section we will first analyze whether the experimental data of the various experimental approaches are compatible with each other. In a second step the uncertainties of additional ingredients for the calculation of the rate factor $N_A < \sigma v >$ will be studied. These are in particular calculated resonance strengths $\omega\gamma$ for the transfer experiments and the theoretically estimated ground-state branching for the reverse reaction experiments. The resulting rate factors $N_A < \sigma v >$ are normalized to the reference factor $N_A < \sigma v >_{\text{ref}}$, determined from the reference cross section σ_{ref} , i.e. the MAT data with all revisions shown in Table II. The results are shown

in Fig. 2. For comparison, a theoretical prediction using the statistical model is also shown [17].

It has to be pointed out here that a comparison between the average cross sections $\bar{\sigma}$ in SAL and the resonance data in MAT and GRO is possible for the first time (see also Fig. 1) because the total widths Γ of the states in ^{22}Mg are now available from Table I.

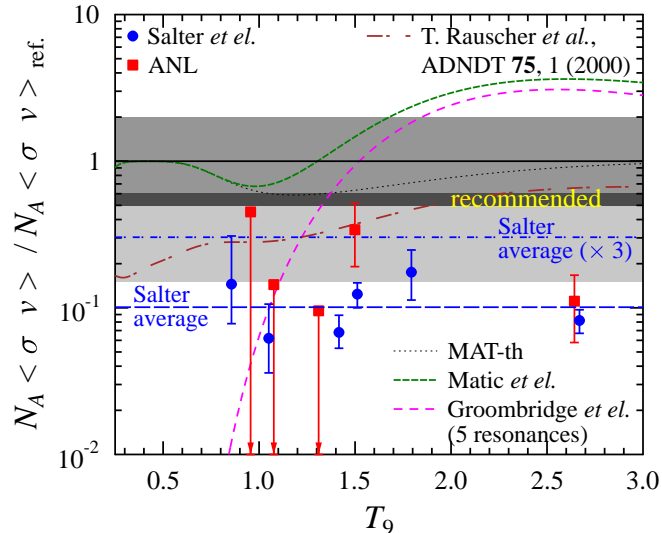


FIG. 2: (Color online) Ratio between the reaction rate factors $N_A \langle \sigma v \rangle$ from different studies normalized to the reference rate factor $N_A \langle \sigma v \rangle_{\text{ref}}$ from the MAT data and the modifications in Table II. Long-dashed magenta line: 5 adopted resonances of the GRO experiment; green short-dashed line: original MAT data; black dotted line: MAT data with calculated strengths $\omega\gamma$ for the 5 resonances of GRO (MAT-th); horizontal blue dashed and dash-dotted lines: average of the SAL data and average multiplied by a factor of three to correct for the ground-state branching. (Color codes and line styles are identical to Fig. 1.) The conversion of the experimental SAL and ANL data to the shown $N_A \langle \sigma v \rangle$ data points is explained in the text. The recommended rate factor $N_A \langle \sigma v \rangle_{\text{recommended}}$ is located in the narrow overlap of the error bars of the reverse reaction data (SAL $\times 3$, lightgrey shaded) and the reference rate (grey shaded) at approx. $0.55 \times N_A \langle \sigma v \rangle_{\text{ref}}$. (dark grey shaded). Numerical values are listed in Table VI. A theoretical prediction in the statistical model is also shown (brown dash-dotted) [17].

A. Are the transfer data compatible with the direct data?

Here a strict comparison of experimental data is limited to excitation energies E^* or resonance energies E which have been determined in the MAT transfer and the GRO direct experiment. 5 of 8 resonances measured by GRO have been uniquely assigned to states which have been seen in the transfer experiment of MAT. Two further resonances have not been seen in the MAT transfer experiment, but have been detected in other transfer ex-

periments (see Table V in MAT). The lowest resonance in GRO is tentatively assigned to a doublet of states in the MAT data. Thus, there is no strict contradiction between the experimental transfer data and the direct data by GRO.

For the calculation of reaction rate factors $N_A \langle \sigma v \rangle$ from Eq. (1) MAT have used the strengths of the 5 uniquely assigned resonances. The remaining 3 resonances of GRO are neglected. However, some other states have been observed by MAT in the energy range of the GRO experiment, and theoretical strengths have been used in MAT for these resonances. Consequently, the calculated $N_A \langle \sigma v \rangle$ of MAT and GRO agree well within the temperature range where the observed resonances in GRO define the rate factor $N_A \langle \sigma v \rangle$ whereas the $N_A \langle \sigma v \rangle$ of GRO is much smaller at lower temperatures (see Fig. 2).

A further compatibility test can be made. The resonance strength $\omega\gamma$ has a general upper limit: $\omega\gamma \leq \omega\Gamma/2$. The total widths Γ vary between 21 and 144 keV for the resonances in GRO [12]. These widths impose an experimental upper limit on the rate factor $N_A \langle \sigma v \rangle$ which is about one order of magnitude above the GRO result. The relatively large strengths in GRO are thus fully compatible, but at the upper limit of the allowed range, especially in the expected case of $\Gamma_\alpha \ll \Gamma_p \approx \Gamma$.

This finding is further strengthened by a theoretical calculation for the only state with a firm spin assignment. The 2^+ state at $E = 2130$ keV has been considered as a member of a $Q = 10$ higher-nodal rotational band in a simple α -cluster model of $^{22}\text{Mg} = ^{18}\text{Ne} \otimes \alpha$ with the semi-magic ($N = 8$) ^{18}Ne core (similar to [18, 19]). Even for well-established α -cluster states in the neighboring nuclei $^{19}\text{F} = ^{15}\text{N} \otimes \alpha$ and $^{20}\text{Ne} = ^{16}\text{O} \otimes \alpha$ with their semi-magic ($N = 8$) or doubly-magic ($N = Z = 8$) cores it has been found that the calculated width Γ_α in this model overestimates the experimental width by at least 30% and often by about a factor of two. Here we find for the 2^+ resonance at 2130 keV an experimental strength of $\omega\gamma = 10.3^{+8.6}_{-1.4}$ keV which corresponds to $\Gamma_\alpha = 2.06^{+1.72}_{-0.28}$ keV for $\Gamma_\alpha \ll \Gamma_p$. The cluster model predicts $\Gamma_\alpha = 1.86$ keV. Again, the experimental results of GRO are at the upper limit of the allowed range.

The same procedure has been repeated for the other 4 resonances from GRO which had entered the original calculation of the rate factor in MAT. The results are listed in Table IV. In all cases the α width derived from the resonance strengths of the GRO experiment are close or even above the theoretical upper limit. This is a very unusual finding. However, because only tentative spin assignments are available for these remaining 4 resonances, it is not possible to strictly exclude the GRO results from the above theoretical considerations. This holds in particular for the $[4^+]$ resonance at 2.287 MeV where the GRO width exceeds the theoretical limit by almost a factor of 10. In this case the reduction factors from Table III suggest $J \leq 2$ to allow for the observed resonance strength of GRO.

TABLE IV: Properties of 5 states in ^{22}Mg from the GRO data and comparison of the derived $\Gamma_\alpha^{\text{GRO}}$ from $\omega\Gamma_\alpha \approx \omega\gamma$ to a theoretically estimated maximum width $\Gamma_\alpha^{\text{th,max}}$ (discussion see text). All energies E are given in MeV; widths Γ and resonance strengths $\omega\gamma$ are given in keV.

E^{GRO}	$E^*\text{GRO}$	Γ^{GRO}	E^{MAT}	$E^*\text{MAT}$	Γ^{MAT}	J^π	$\omega\gamma^{\text{GRO}}$	$\Gamma_\alpha^{\text{GRO}}$	$\Gamma_\alpha^{\text{th,max}}$
2.17±0.14	10.312	130±80	2.130	10.272	21±3	2 ⁺	10.3 ^{+8.6} _{-1.4}	2.06 ^{+1.72} _{-0.28}	1.87
2.28±0.15	10.422	210±100	2.287	10.429	144±26	[4 ⁺]	7.3 ^{+9.7} _{-1.5}	0.81 ^{+1.08} _{-0.17}	0.093
2.52±0.14	10.662	100±50	2.509	10.651	73±19	[3 ⁻]	18.2 ^{+8.9} _{-1.9}	2.60 ^{+1.27} _{-0.27}	1.81
2.72±0.14	10.862	210±10	2.731	10.873	40±12	[0 ⁺]	45.2 ^{+14.6} _{-11.8}	45.2 ^{+14.6} _{-11.8}	97.1
2.87±0.14	11.012	100±20	2.859	11.001	136±13	[4 ⁺]	8.1 ^{+2.9} _{-2.0}	0.90 ^{+0.32} _{-0.22}	1.23

B. Are the transfer data compatible with the reverse reaction data?

A direct comparison between the MAT excitation energies and resonance strengths and the SAL average cross sections is difficult because there are no common observables in the different experimental approaches. Nevertheless, a comparison can be made in the following way. From Eq. (4) and $\sigma_{\text{ref.}}(E)$, see Sect. II A 1, the average cross section $\bar{\sigma}(\alpha, p)$ can be calculated for each data point of SAL and ANL. These calculated $\bar{\sigma}(\alpha, p)$ should be about a factor of ≈ 3 larger because the reverse reaction data determine only the ground-state contribution (α, p_0). The factor of ≈ 3 is taken from the HF calculations in SAL (see also discussion in Sect. II C 1). The results are listed in Table V.

TABLE V: Average cross sections $\bar{\sigma}(\alpha, p)$ from $\sigma_{\text{ref.}}(E)$ compared to the SAL and ANL data. Further discussion see text.

$E_{\text{eff}}(\alpha, p)$ (MeV)	exponent for σ in mb	σ_{exp}	Ref.	$\bar{\sigma}_{\text{ref.}}$	$\sigma_{\text{exp}}/\bar{\sigma}_{\text{ref.}}$
1.194±0.130	10 ⁻⁴	5.5 ^{+6.2} _{-3.5}	SAL	37.8	0.145 ^{+0.164} _{-0.067}
1.379±0.129	10 ⁻³	3.8 ^{+2.7} _{-1.6}	SAL	61.6	0.062 ^{+0.044} _{-0.026}
1.683±0.121	10 ⁻²	2.3 ^{+0.7} _{-0.5}	SAL	33.7	0.068 ^{+0.021} _{-0.015}
1.758±0.069	10 ⁻²	3.1 ± 0.6	SAL	25.1	0.124 ± 0.024
1.970±0.117	10 ⁻¹	1.7 ^{+0.7} _{-0.6}	SAL	9.7	0.175 ^{+0.073} _{-0.062}
2.568±0.061	10 ⁰	1.7 ± 0.3	SAL	20.7	0.082 ± 0.015
1.748±0.077	10 ⁻²	7.5 ^{+3.8} _{-3.3}	ANL	22.0	0.341 ^{+0.173} _{-0.150}
2.551±0.077	10 ⁰	2.0 ^{+1.0} _{-0.9}	ANL	17.8	0.111 ^{+0.056} _{-0.053}

The ratios $\sigma_{\text{exp}}/\bar{\sigma}_{\text{ref.}}$ vary between 0.06 and 0.15 for the SAL data with a geometric mean of 0.101. The higher energy data point of the ANL data is in good agreement with the corresponding SAL data point with a ratio of 0.11 compared to 0.08 from SAL. The lower point of ANL is slightly higher by a factor of about 2.5 but has an uncertainty of a factor of two. The upper limits of the ANL data are compatible with the SAL data points at lower energies. Thus, in general the experimental data of SAL and ANL are in reasonable agreement.

As pointed out above (see Sec. II C), a calculation of reaction rate factors $N_A < \sigma v >$ from experimental cross sections with relatively large uncertainties in the energy may have large uncertainties and thus may be misleading. Here we estimate the rate factors from the reverse reaction experiments in the following way. We adopt the en-

ergy dependence of $\sigma_{\text{ref.}}(E)$ and use the ratio $\sigma_{\text{exp}}/\bar{\sigma}_{\text{ref.}}$:

$$N_A < \sigma v >_{\text{exp}}(T) = N_A < \sigma v >_{\text{ref.}}(T) \times \frac{\sigma_{\text{exp}}(E)}{\bar{\sigma}_{\text{ref.}}(E)} \quad (5)$$

The temperature T for each data point is taken from the most effective energy E_{eff} of the Gamow window which is given by the well-known relation $E_{\text{eff}}/\text{keV} = 122 \times (Z_P^2 Z_T^2 A_{\text{red}} T_9^2)^{1/3}$. This leads to the experimental data points shown in Fig. 2. Their average value is almost exactly a factor of 10 lower than the reference rate $N_A < \sigma v >_{\text{ref.}}$ (horizontal blue dashed line in Fig. 2). Because of the experimental uncertainties of the SAL and ANL data, a better determination of the temperature dependence of the rate factor $N_A < \sigma v >$ from experimental data for the reverse reaction is not possible.

A strict comparison of $\bar{\sigma}_{\text{ref.}}$ and σ_{exp} requires two theoretical considerations. First, calculated resonance strengths $\omega\gamma$ have been used in the calculation of $\sigma_{\text{ref.}}(E)$, and, second, the calculated ground-state branching of about one third (as suggested in SAL, see also Sect. II C 1) is responsible for an expected factor of three discrepancy between $\bar{\sigma}_{\text{ref.}}$ and σ_{exp} . However, the ratio $\sigma_{\text{exp}}/\bar{\sigma}_{\text{ref.}}$ turns out to be about 0.1 (see Table V); i.e., it is a further factor of three smaller than expected. Both calculations ($\omega\gamma$ for the transfer data, the ground state branching for the reverse reaction data) are based on simple but reasonable arguments, and the uncertainties should not exceed a factor of two. This factor of two for the uncertainties of $N_A < \sigma v >_{\text{ref.}}$ and $N_A < \sigma v >$ from the reverse reaction data are shown as shaded areas in Fig. 2. Thus, the real rate can be estimated as follows.

From the transfer data the reference rate $N_A < \sigma v >_{\text{ref.}}$ is derived with an uncertainty of a factor of two; i.e., the real rate should be located in the interval between $0.5 \times N_A < \sigma v >_{\text{ref.}}$ and $2.0 \times N_A < \sigma v >_{\text{ref.}}$. From the reverse reaction the best estimate for the real rate is $0.3 \times N_A < \sigma v >_{\text{ref.}}$ (taking into account the ground state branching of about 1/3 as discussed above), again with an uncertainty of about a factor of two; i.e., the real rate should be located in the interval between $0.15 \times N_A < \sigma v >_{\text{ref.}}$ and $0.6 \times N_A < \sigma v >_{\text{ref.}}$. Combining the above intervals, for the real rate only a narrow window around $(0.5 - 0.6) \times N_A < \sigma v >_{\text{ref.}}$ remains to be compatible with all experimental results. Uncertainties for this finally recommended rate will be given in Sect. IV.

C. Are the direct data compatible with the reverse reaction data?

A strict comparison between the direct GRO data and the reverse reaction data is possible because GRO have determined the main decay branch of the resonances seen in their experiment. In particular, according to GRO, a resonance at 2.52 ± 0.14 MeV with a width of $\Gamma = 100 \pm 50$ keV decays mainly to the p_0 channel with a resonance strength of $\omega\gamma = 18.2^{+8.9}_{-1.9}$ keV. MAT have assigned $J^\pi = [3^-]$, $E = 2.509 \pm 0.013$ MeV, and $\Gamma = 73 \pm 19$ keV. The experimental data points at the highest energies of the SAL and ANL data around 2.5 MeV are affected by this resonance. Using the resonance energy E from MAT, the total width from the MAT experiment (see Table I), and the resonance strength $\omega\gamma$ from GRO, we find $\bar{\sigma} = 40.2$ mb for the SAL data point at 2.568 MeV which is a factor of 24 higher than the experimental value of 1.7 ± 0.3 mb. A similar factor of 23 is found for the ANL data point of $2.0^{+1.0}_{-0.9}$ mb where $\bar{\sigma} = 45.3$ mb is calculated. A much better agreement is found if the huge resonance strength of $\omega\gamma = 18.2$ keV from the GRO data is replaced by the calculated strength of $\omega\gamma = 1.12$ keV (see Table II): $\bar{\sigma} = 2.47$ mb for the SAL data point and 2.79 mb for the ANL data point. The role of this resonance turns out to be minor for the total reaction cross section (see Fig. 1) which is dominated by the long tail of the strong 0^+ resonance at 2.731 MeV.

This leads to the clear conclusion that there is a strict contradiction between the experimental data of GRO in the direct experiment and the experimental SAL data using the reverse reaction. This conclusion is independent of any theoretical calculations. It seems more likely that there is an experimental problem in the normalization of the GRO data because the unpublished ANL data for the reverse reaction are in agreement with the SAL data, and thus there must be a problem in the two independent SAL and ANL experiments if the GRO data are correct.

IV. RECOMMENDED REACTION RATE FACTOR $N_A \langle \sigma v \rangle$

The above discussion leads to the following recommendations for the reaction rate factor $N_A \langle \sigma v \rangle$ of the $^{18}\text{Ne}(\alpha, p)^{21}\text{Na}$ reaction. The most realistic estimate from the overlap of the uncertainties in Fig. 2 is located around $0.55 \times N_A \langle \sigma v \rangle_{\text{ref.}}$. Consequently, this rate factor is recommended for further use in astrophysical calculations. Numerical values are listed in Table VI.

Uncertainties for $N_A \langle \sigma v \rangle$ may be estimated as follows. A realistic lower limit can be taken from the SAL data (multiplied by a factor of three to take into account the ground-state branching) which is shown as a blue dash-dotted line in Fig. 2. A realistic upper limit is the reference rate factor $N_A \langle \sigma v \rangle_{\text{ref.}}$. A strict lower limit provide the SAL data (without the correction of the ground-state branching, see blue dashed line in Fig. 2).

TABLE VI: Recommended rate factor $N_A \langle \sigma v \rangle_{\text{recommended}}$ in $\text{cm}^3 \text{s}^{-1} \text{mol}^{-1}$ and realistic lower and upper limits. Note that $N_A \langle \sigma v \rangle_{\text{recommended}} = 0.55 \times N_A \langle \sigma v \rangle_{\text{ref.}}$. The lower limit is given by $0.30 \times N_A \langle \sigma v \rangle_{\text{ref.}}$, and the upper limit is given by $N_A \langle \sigma v \rangle_{\text{ref.}}$.

T_9	recommended	lower	upper
0.1	4.1×10^{-24}	2.3×10^{-24}	7.5×10^{-24}
0.2	1.7×10^{-15}	9.6×10^{-16}	3.2×10^{-15}
0.3	3.0×10^{-11}	1.6×10^{-11}	5.4×10^{-11}
0.4	1.1×10^{-08}	6.1×10^{-09}	2.0×10^{-08}
0.5	7.2×10^{-07}	4.0×10^{-07}	1.3×10^{-06}
0.6	1.7×10^{-05}	9.3×10^{-06}	3.1×10^{-05}
0.7	2.1×10^{-04}	1.1×10^{-04}	3.8×10^{-04}
0.8	1.7×10^{-03}	9.3×10^{-04}	3.1×10^{-03}
0.9	1.0×10^{-02}	5.7×10^{-03}	1.9×10^{-02}
1.0	4.8×10^{-02}	2.7×10^{-02}	8.8×10^{-02}
1.1	1.8×10^{-01}	1.0×10^{-01}	3.3×10^{-01}
1.2	5.7×10^{-01}	3.2×10^{-01}	$1.0 \times 10^{+00}$
1.3	$1.5 \times 10^{+00}$	8.5×10^{-01}	$2.8 \times 10^{+00}$
1.4	$3.7 \times 10^{+00}$	$2.0 \times 10^{+00}$	$6.7 \times 10^{+00}$
1.5	$8.0 \times 10^{+00}$	$4.4 \times 10^{+00}$	$1.5 \times 10^{+01}$
1.6	$1.6 \times 10^{+01}$	$8.9 \times 10^{+00}$	$2.9 \times 10^{+01}$
1.7	$3.0 \times 10^{+01}$	$1.7 \times 10^{+01}$	$5.5 \times 10^{+01}$
1.8	$5.4 \times 10^{+01}$	$3.0 \times 10^{+01}$	$9.8 \times 10^{+01}$
1.9	$9.1 \times 10^{+01}$	$5.0 \times 10^{+01}$	$1.7 \times 10^{+02}$
2.0	$1.5 \times 10^{+02}$	$8.3 \times 10^{+01}$	$2.7 \times 10^{+02}$
2.1	$2.4 \times 10^{+02}$	$1.3 \times 10^{+02}$	$4.3 \times 10^{+02}$
2.2	$3.7 \times 10^{+02}$	$2.0 \times 10^{+02}$	$6.7 \times 10^{+02}$
2.3	$5.6 \times 10^{+02}$	$3.1 \times 10^{+02}$	$1.0 \times 10^{+03}$
2.4	$8.2 \times 10^{+02}$	$4.5 \times 10^{+02}$	$1.5 \times 10^{+03}$
2.5	$1.2 \times 10^{+03}$	$6.6 \times 10^{+02}$	$2.2 \times 10^{+03}$
2.6	$1.7 \times 10^{+03}$	$9.3 \times 10^{+02}$	$3.1 \times 10^{+03}$
2.7	$2.4 \times 10^{+03}$	$1.3 \times 10^{+03}$	$4.3 \times 10^{+03}$
2.8	$3.3 \times 10^{+03}$	$1.8 \times 10^{+03}$	$6.0 \times 10^{+03}$
2.9	$4.5 \times 10^{+03}$	$2.5 \times 10^{+03}$	$8.1 \times 10^{+03}$
3.0	$6.0 \times 10^{+03}$	$3.3 \times 10^{+03}$	$1.1 \times 10^{+04}$

A strict upper limit in the astrophysically most relevant temperature range is about a factor of three higher than the reference rate factor. It can be taken from the GRO results; although these results seem to be questionable, it has been shown that the GRO strengths are close to theoretical upper limits and thus suitable to provide an upper limit.

Finally, this leads to a recommended reaction rate factor $N_A \langle \sigma v \rangle_{\text{recommended}} = 0.55 \times N_A \langle \sigma v \rangle_{\text{ref.}}$ with a realistic uncertainty of a factor of 1.8 and an extreme uncertainty of a factor of 5.5; it is interesting to note that after all the estimates of uncertainties one ends up with an almost Gaussian uncertainty distribution with a factor of 1.8 for a realistic (1 sigma) uncertainty and a factor of about 5.5 for an extreme uncertainty (3 sigma).

Of course, the reduction factor of 0.55 between the reference calculations and the final recommended rate factor also has to be applied to the reference cross section $\sigma_{\text{ref.}}$ shown in Fig. 1. The absolute value of $\sigma_{\text{ref.}}$ depends on the calculated resonance strengths $\omega\gamma$ which are proportional to the decay widths Γ_α into the α channel (for $\Gamma_\alpha \ll \Gamma_p$). Thus, all calculated Γ_α of MAT and in Table

II should be reduced by the same factor of 0.55.

The recommended rate factor $N_A < \sigma v >_{\text{recommended}}$ is slightly lower than the MAT rate factor around $T_9 \approx 1$, but significantly smaller at higher temperatures around $T_9 \approx 2$. The minor difference between the MAT rate factor and $N_A < \sigma v >_{\text{recommended}}$ at lower temperatures is due to a compensation of the enhancement from new spin assignments from the CHA transfer data (leading to smaller spins J and thus increased resonance strengths) and the derived reduction factor of 0.55 from the comparison with the reverse reaction data. The significant decrease at higher temperatures is mainly a consequence of the replacement of the huge resonance strengths from the GRO experiment by smaller calculated resonance strengths.

In a comparison of the new recommended rate factor $N_A < \sigma v >_{\text{recommended}}$ with the SAL result (see Table II in [5]) it has to be kept in mind that SAL provide the rate factor for the ground-state contribution $^{18}\text{Ne}(\alpha, p_0)^{21}\text{Na}_{\text{g.s.}}$ which is derived from their experimental data; the given upper and lower limits are calculated from their experimental uncertainties, but do not include the additional contributions of the $(\alpha, p_{i \neq 0})$ channels and the corresponding uncertainties. Thus, it is not surprising that the new recommended rate factor exceeds the upper limit of the SAL rate factor. The new recommended rate factor is about a factor of 5 higher than the SAL result in the astrophysically most relevant temperature range of $T_9 = 1 - 2$.

The theoretical prediction of the $^{18}\text{Ne}(\alpha, p)^{21}\text{Na}$ cross section in [17] is based on the statistical model and a global parameter set. The calculation has been done before the experimental results of GRO, SAL, MAT, ANL, CHA, and MAT were available. By definition, such a statistical model calculation cannot reproduce details of the $\sigma(E)$ curve shown in Fig. 1. Nevertheless, the predicted rate factor $N_A < \sigma v >$ is in reasonable agreement with the recommended rate factor (see Fig. 2) and remains within the realistic uncertainty estimate of $N_A < \sigma v >_{\text{recommended}}$ in the temperature range $T_9 = 1 - 3$. However, the temperature dependence of the theoretical rate factor is slightly steeper compared to the recommended rate factor, and thus at low temperatures below $T_9 \approx 1$ the theoretical rate factor is located below the recommended rate factor between the realistic and the extreme lower limit of the recommendation.

The recommended rate factor $N_A < \sigma v >_{\text{recommended}}$ is fitted by the usual expression, see e.g. [17], Eq. (16):

$$\frac{N_A < \sigma v >}{\text{cm}^3 \text{s}^{-1} \text{mol}^{-1}} = \exp(a_0 + a_1 T_9^{-1} + a_2 T_9^{-1/3} + a_3 T_9^{1/3} + a_4 T_9 + a_5 T_9^{5/3} + a_6 \ln T_9) \quad (6)$$

The a_i parameters are listed in Table VII. The deviation of the fitted rate factor is always below 10% over the full temperature range $0.25 \leq T_9 \leq 3$ and typically below 5% in the most relevant range $1 \leq T_9 \leq 2$.

V. SUMMARY AND CONCLUSIONS

The present knowledge of the reaction rate factor $N_A < \sigma v >$ of the $^{18}\text{Ne}(\alpha, p)^{21}\text{Na}$ reaction has been summarized. For this purpose experimental results from different experimental techniques are combined. Transfer reactions provide the best determination of the excitation energy E^* and spin and parity J^π of states in ^{22}Mg which appear as resonances in the $^{18}\text{Ne}(\alpha, p)^{21}\text{Na}$ reaction; however, transfer reactions cannot provide the required resonance strengths $\omega\gamma$. These strengths have to be taken from theory or from direct experiments which are however extremely difficult and require the combination of a radioactive ^{18}Ne beam and a helium gas target. Complementary information has been derived from the experimental study of the reverse $^{21}\text{Na}(p, \alpha)^{18}\text{Ne}$ reaction using a radioactive ^{21}Na beam and a solid CH_2 target.

A basic prerequisite for the comparison of results from various experimental techniques is the availability of total widths Γ for the resonances under study. The total widths Γ were determined from a reanalysis of the peak widths in the MAT experiment.

A compatibility test between the results from various experimental techniques shows that there is no contradiction between the various experimental data except the disagreement between the direct GRO data and the reverse reaction data from SAL and ANL. This leads to the conclusion that the most likely explanation is a problem in the normalization of the GRO data. Consequently, resonance strengths from GRO have been replaced by theoretical resonance strengths in the calculation of the rate factor $N_A < \sigma v >$.

The calculation of $N_A < \sigma v >$ for the $^{18}\text{Ne}(\alpha, p)^{21}\text{Na}$ reaction from transfer data requires theoretical resonance strengths, and the calculation of $N_A < \sigma v >$ from the reverse $^{21}\text{Na}(p, \alpha)^{18}\text{Ne}$ reaction data requires a theoretical estimate of the (α, p_0) ground-state branching. Both calculations are based on simple but reasonable arguments, and the corresponding uncertainties should not exceed a factor of two. This leads to a relatively narrow overlap region between the higher $N_A < \sigma v >$ calculated from transfer and the lower $N_A < \sigma v >$ calculated from the reverse reaction data. This narrow overlap region is considered as the new recommended reaction rate factor $N_A < \sigma v >_{\text{recommended}}$. The uncertainty of the recommended rate factor is about a factor of 1.8 ($\approx 1 \sigma$ uncertainty). For $T_9 = 1 - 3$ a theoretical prediction [17] lies within this error band, but the theoretical temperature dependence of the rate factor $N_A < \sigma v >$ is somewhat steeper than the new recommendation.

The new recommended rate factor is slightly lower than the MAT rate factor at low temperatures and significantly smaller at higher temperatures, and the new rate factor exceeds the SAL result by about a factor of 5. The strong conclusion of SAL (based on their lower limit for the rate factor $N_A < \sigma v >$) that “the breakout from the HCNO cycle via the $^{18}\text{Ne}(\alpha, p)^{21}\text{Na}$ reaction is delayed and occurs at higher temperatures than previously

TABLE VII: Fit parameters a_i of the reaction rate factor $N_A \langle \sigma v \rangle$ from Eq. (6).

a_0	a_1	a_2	a_3	a_4	a_5	a_6
-21.0595	-0.3301	-58.1167	89.3359	-14.8713	1.9862	-24.1080

predicted” cannot be supported. Instead, because of the only minor deviations of $N_A \langle \sigma v \rangle_{\text{recommended}}$ from the MAT result at low temperatures around $T_9 = 1$, the earlier conclusions of MAT should remain valid in general. Further astrophysical network calculations with the new recommended rate factor $N_A \langle \sigma v \rangle_{\text{recommended}}$ are required to study the relevance of the modified temperature dependence of the rate factor in detail.

Acknowledgments

We thank M. Aliotta, A. M. van den Berg, G. P. A. Berg, K.-E. Rehm, P. Salter, M. Wiescher for encouraging discussions, and T. Rauscher for his code EXP2RATE. This work was supported by OTKA (NN83261).

-
- [1] H. Schatz and K. E. Rehm, Nucl. Phys. **A777**, 601 (2006).
- [2] M. Wiescher, J. Görres, H. Schatz, J. Phys. G **25**, R133 (1999).
- [3] W. Bradfield-Smith *et al.*, Phys. Rev. C **59**, 3402 (1999).
- [4] D. Groombridge *et al.*, Phys. Rev. C **66**, 055802 (2002).
- [5] P. J. C. Salter *et al.*, Phys. Rev. Lett. **108**, 242701 (2012).
- [6] S. Sinha *et al.*, ANL Annual Report 2005, p.6-7.
- [7] A. A. Chen, R. Lewis, K. B. Swartz, D. W. Visser, P. D. Parker, Phys. Rev. C **63**, 065807 (2001).
- [8] J. A. Caggiano *et al.*, Phys. Rev. C **66**, 015804 (2002).
- [9] G. P. A. Berg *et al.*, Nucl. Phys. **A718**, 608 (2003).
- [10] K. Y. Chae *et al.*, Phys. Rev. C **79**, 055804 (2009).
- [11] A. Matic *et al.*, Phys. Rev. C **80**, 055804 (2009).
- [12] A. Matic, PhD thesis, Rijksuniversiteit Groningen, 2007; available online at <http://dissertations.ub.rug.nl/faculties/science/2007/>.
- [13] <http://www-nds.iaea.org/amdc/>; G. Audi, F. G. Kondev, M. Wang, B. Pfeiffer, X. Sun, J. Blachot, M. MacCormick, Chin. Phys. C **36**, 1157 (2012); G. Audi, M. Wang, A. H. Wapstra, F. G. Kondev, M. MacCormick, X. Xu, B. Pfeiffer, Chin. Phys. C **36**, 1287 (2012); M. Wang, G. Audi, A. H. Wapstra, F. G. Kondev, M. MacCormick, X. Xu, B. Pfeiffer, Chin. Phys. C **36**, 1603 (2012).
- [14] G. Audi, A. H. Wapstra, C. Thibault, Nucl. Phys. **A729**, 337 (2003).
- [15] B. A. Brown and B. H. Wildenthal, Ann. Rev. Nucl. Part. Sci. **38**, 29 (1988); B. A. Brown, <http://www.nscl.msu.edu/~brown/resources/resources.html>.
- [16] T. Rauscher, EXP2RATE v2.1 (<http://nucastro.org/codes.html>).
- [17] T. Rauscher and F.-K. Thielemann, At. Data Nucl. Data Tables **75**, 1 (2000).
- [18] H. Abele and G. Staudt, Phys. Rev. C **47**, 742 (1993).
- [19] S. Wilmes, V. Wilmes, G. Staudt, P. Mohr, J. W. Hammer, Phys. Rev. C **66**, 065802 (2002).